

# Moving towards circular economy: REE recovery from secondary sources exploiting zeolites cation exchange properties

Francesco Colombo

Department of Chemical and Geological Sciences, University of Modena and Reggio Emilia, Via G. Campi 103, 41125, Modena

DOI: 10.19276/plinius.2025.01.007

## INTRODUCTION

Rare Earth Elements (REEs) comprise a group of 17 elements, including the 15 lanthanides (atomic numbers 57-71) plus scandium (Sc) and yttrium (Y). These elements are typically divided into light rare earth elements (LREEs: La-Gd) and heavy rare earth elements (HREEs: Tb-Lu) based on their electron configurations and atomic masses. Most REEs predominantly form trivalent ions ( $\text{RE}^{3+}$ ), though cerium can also exist as  $\text{Ce}^{4+}$  and europium as  $\text{Eu}^{2+}$  under specific conditions. The most economically significant REE deposits include the Bayan Obo deposit in China, considered the world's largest REE deposit (Huang et al., 2015; Smith et al., 2016; Song et al., 2018; Dushyantha et al., 2020), the Mountain Pass deposit (USA), a carbonatite-hosted deposit rich in bastnäsite (Castor, 2008), Mount Weld (Australia), notable for its high-grade REE concentrations (Lottermoser et al., 1988; Lottermoser, 1990; Jaireth et al., 2014) and Ion Adsorption Clays (Southern China), formed from weathered granites, particularly important for HREE production due to their ease of extraction (Borst et al., 2020; Feng et al., 2021). Other significant deposits exist in Brazil, Russia, and Africa, often associated with alkaline complexes or carbonatites. Global REE production in 2023 reached approximately 350,000 metric tons, with China responsible for ~68.5% of the output. The U.S. (Mountain Pass) and Myanmar have also become key producers. Total global reserves are estimated at ~110 million tonnes of REO, with major deposits in China, Vietnam, and Brazil (U.S. Geological Survey, 2024). REE mining and processing pose significant environmental challenges. Among the others, the mining process generates dust, habitat destruction, and acid mine drainage; the processing requires strong acids ( $\text{H}_2\text{SO}_4$ , HCl) and produces toxic byproducts (e.g., thorium in Baotou tailings). Extraction from Ion Adsorption Clays, while less damaging, still requires ammonium sulphate leaching, which can contaminate groundwater. The European Union classifies REEs as critical raw materials due to their economic importance and supply risks, as the region currently imports

nearly all its REEs (Grohol & Veeh, 2023). The importance of these elements is strongly related to their indispensable role in numerous advanced technological applications that define modern life. Their unique magnetic and luminescent properties make them particularly valuable in clean energy technologies, such as high-performance permanent magnets used in electric vehicle motors and wind turbine generators. With the global transition toward renewable energy and electrified transportation, demand for these strategically important elements has been growing exponentially. This surge in demand underscores both the critical importance of rare earth elements in modern technology and the need for secure, responsible supply chains to meet future requirements. Recycling REEs from end-of-life products (e.g., magnets, batteries), or from other typologies of wastes (e.g., WEEE) is becoming increasingly important to supplement primary production and reduce environmental impacts. Potential secondary sources include industrial mining byproducts like phosphogypsum, red mud and coal ash, and electronic waste (WEEE) such as NdFeB magnets, NiMH batteries and fluorescent lamp phosphors. Effective separation of Rare Earth Elements (REEs) from leachates - deriving from waste materials - employs several possible methods such as selective precipitation, solvent extraction, selective adsorption (e.g., with activated carbon, biochar, or functionalized resins), ion exchange exploiting resins or Metal-Organic Frameworks (MOFs). Zeolites—particularly faujasite-types (X and Y, differing in Si/Al ratio)—can be exploited for their cation exchange property for REE recovery. Recent studies highlight zeolites' potential in REE separation from waste streams, leveraging their pore structure and exchange properties. This work is a feasibility study aimed at evaluating the efficiency of recovery of REEs from waste solutions, exploiting the cation exchange property of zeolites. These materials have the potential to be a reusable and selective method for the separation of REEs. In particular, a  $\text{NH}_4$ -exchanged zeolite 13X was prepared to facilitate the further recovery of REEs from the zeolite. In

fact, the procedure we propose is a two-step exchange: *i)*  $\text{NH}_4$ -exchanged 13X is contacted with REE solution to promote the extraction of selected REE from the solution through a REE- $\text{NH}_4$  exchange; *ii)* the REE-exchanged zeolites are then contacted with an  $\text{NH}_4$  solution to extract the REE. The presence of only  $\text{NH}_4$  in the zeolites, in fact, simplifies the final REE recovery, allowing a selective precipitation as nitrates. The waste solutions used in this work are lab-made solutions mimicking the products obtained from the leaching of spent fluorescent lamps, a complex secondary source of rare earth elements (REEs), containing valuable metals such as yttrium, europium, terbium, cerium, and lanthanum.

## MATERIALS AND METHODS

### 13X zeolite

Faujasite-type zeolites (FAU) have a highly porous cubic structure composed of sodalite cages and double 6-rings, forming large supercages with  $\sim 7.5$  Å openings. Variants X and Y differ by Si/Al ratio: faujasite X, with a lower Si/Al ratio, offers higher cation-exchange capacity but lower acid stability. For this work, the starting material NaX zeolite was selected for its ion-exchange potential. The zeolites were then  $\text{NH}_4$ -exchanged. The presence of  $\text{NH}_4$  as the only extra-framework cation would help in the further exchange required for the REE recovery, enabling separation of REEs via pH-controlled precipitation, as  $\text{NH}_4^+$  remains soluble while REEs form insoluble hydroxides. Full sodium substitution was nevertheless not achieved.

### Mono- and bi-elemental exchanges

Mono- and bi-elemental exchange tests were carried out using  $\text{NH}_4$ -exchanged 13X zeolite and REE solutions mimicking concentrations found in leachates of spent fluorescent lamps (Eduafó et al. 2015): Ce (0.03 M), La (0.04 M), Eu (0.006 M), and Y (0.17 M). Mono-elemental tests involved contacting the zeolite with individual REE solutions at three different liquid-to-solid (L/S) ratios (10:1, 50:1, and 100:1 mL/g) for 24 h under stirring at room temperature. Bi-elemental tests were performed using Ce-La and Y-Eu mixed solutions at the same con-

centrations of the mono-elemental solutions, with a fixed L/S ratio and a shorter contact time of 3 h, as the first REE exchange allowed to understand that the equilibrium was quickly achieved. Buffered pH conditions ( $\sim 4.4$ – $4.8$ ) were maintained to avoid zeolite degradation and REE precipitation. Elemental analysis, thermogravimetric analysis, SEM-EDS, XRPD and ICP-MS analyses were performed on the sample obtained. Selected samples after mono-elemental exchanges were analysed by high-resolution XRPD at ESRF for phase and structural characterization.

### REEs recovery from zeolite

REEs were recovered from the exchanged 13X zeolites through a secondary exchange with  $\text{NH}_4\text{Cl}$  solutions. Zeolites from mono-elemental tests were treated with 0.8 M  $\text{NH}_4\text{Cl}$  for 24 h ( $\text{L/S} = 1/125$  g/mL), while those from bi-elemental tests were treated with 1 M  $\text{NH}_4\text{Cl}$  for 3 h ( $\text{L/S} = 1/100$  g/mL), both under stirring at room temperature. The higher  $\text{NH}_4\text{Cl}$  concentration for bi-elemental samples was chosen to improve REE recovery. Elemental analysis, thermogravimetric analysis, SEM-EDS, XRPD and ICP-MS analyses were performed on the sample obtained. Selected samples after mono-elemental exchanges were analysed by high-resolution XRPD at ESRF for phase and structural characterization.

## RESULTS AND DISCUSSION

### Mono- and bi-elemental exchanges

REE uptake from mono-elemental solutions is shown in Figure 1a. At low liquid-to-solid ratios (10 mL/g), Ce, La, and Eu are nearly fully extracted, while Y shows lower uptake ( $\sim 60\%$ ). Increasing the solution volume reduces extraction efficiency for Ce, La, and Y, but not for Eu. REE loading on the zeolite (Fig. 1b) increases with the increase in the liquid/solid ratio, reaching 150–160 mg/g for Ce and La, and  $\sim 75$  mg/g for Y. For all the systems at liquid/solid ratio higher than 50 a plateau is achieved, indicating the approaching of cation exchange saturation. Y uptake plateaus at values inferior to the other REEs tested, despite being the most concentrated in the starting solution, suggesting lower affinity. The zeolite Si/Al

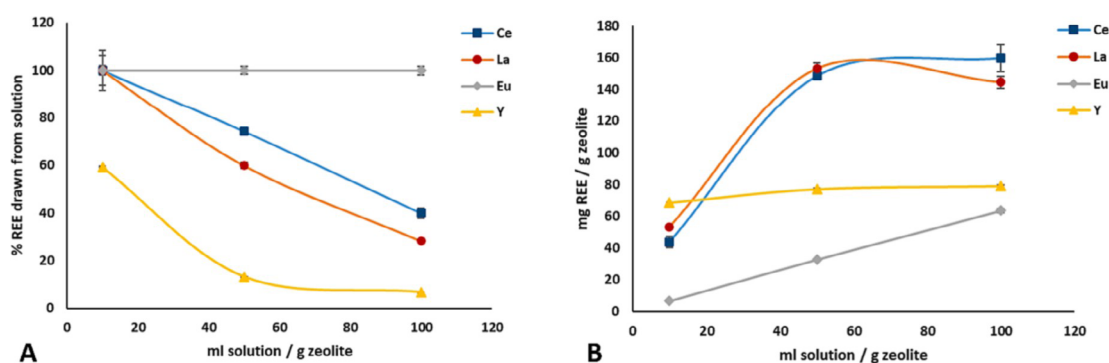
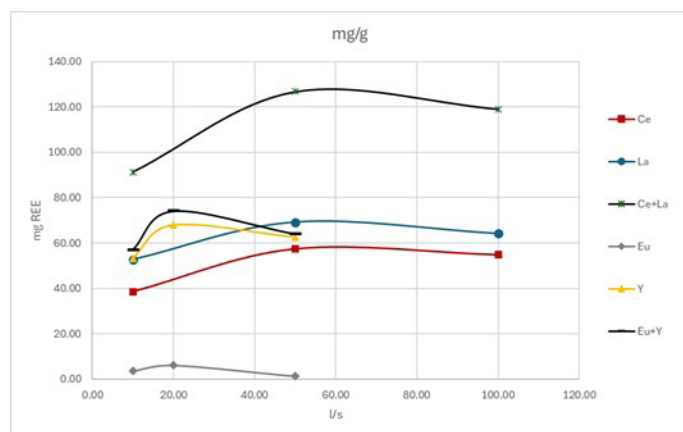


Figure 1 a) REE fraction drawn from solution as a function of the solid/liquid ratio. b) Amount of REE incorporated in the zeolite as a function of the solid/liquid ratio.



**Figure 2** Amount of REE incorporated in the zeolite as a function of the solid/liquid ratio. REEs are also reported in the graph individually, to allow a clearer view of the exchange behaviours of the bi-elemental exchanges. The lines are guides for the eye.

ratio (1.23) remains stable post-exchange. The extent of extra-framework aluminium (EFAL) correlates inversely with REE content; high REE loading stabilizes the framework, echoing behavior seen in REE-Y catalysts in FCC applications (Vogt & Weckhuysen, 2015). Exchange data show that REEs preferentially replace  $\text{NH}_4^+$  rather than  $\text{Na}^+$  left in the channels, as a demonstration that  $\text{Na}^+$  is hardly exchangeable.  $\text{NH}_4^+$  content decreases linearly with REE loading, while  $\text{Na}^+$  remains constant until high REE exchange levels are reached. The results of bi-elemental REE exchange experiments reveal behaviours consistent with mono-elemental tests, while highlighting the influence of inter-element competition and solution concentration (Fig. 2). At low liquid-to-solid (l/s) ratios (e.g., 10), Ce and La are almost fully extracted from solution (~100%), but efficiency decreases with increasing l/s, dropping to ~30% at l/s = 50 and below 20% at l/s = 100. This suggests optimal exchange occurs between l/s = 10–50. La is exchanged more efficiently than Ce (70 vs. 60 mg/g), in line with its higher starting concentration. For the Eu+Y system, REE uptake is limited regardless of l/s ratio: more than 50% of Y remains unexchanged at l/s = 10, and over 90% at l/s = 50. Eu uptake drops to ~60% at l/s = 10 and falls below 5% at higher l/s ratios. Nevertheless, Y dominates the exchange process due to its higher concentration in the starting solution (0.17 M vs. 0.006 M Eu). The total REE exchange capacity remains consistent with mono-elemental data, reaching ~130 mg/g (Ce+La) and ~80 mg/g (Y+Eu). Starting concentration appears to be the dominant factor in competitive uptake.

### REEs recovery after mono- and bi-elemental exchanges

Two consistent trends emerge from both mono- and bi-elemental exchange tests: Y is partially recovered (45%), while Ce, La and Eu show significantly lower recoveries (10–18%), indicating a stronger retention of the latter in the 13X framework. This behaviour is linked to

charge balance variation; greater imbalance after recovery of Y suggests weaker stabilization and easier displacement, while Ce, La and Eu induce minimal charge variation, pointing to stronger binding. Y consistently displays the highest exchangeability, confirming its distinct behaviour and easier removal.

### XRPD analyses

The structural behaviour of selected REE-bearing zeolites after mono-elemental exchanges was investigated via Rietveld structural refinement and compared with the literature. Diffraction data reveal significant differences in peak intensity ratios among the REE-exchanged samples, indicating different electronic densities in relation to the cations exchanged. Ce and La preferentially occupy site II\* (after Frising & Leflaive, 2008) (in the supercage), near the hexagonal window of the sodalite cage (see Fig. 3), and partially share site I' (in the sodalite cage) with  $\text{Na}^+$ . These cations coordinate both framework oxygens and water molecules. Eu exhibits similar site preferences but with lower incorporation, likely due to its lower starting concentration. Y shows distinct behavior, predominantly occupying site IV in the supercage and the sodalite cage in site I', coordinating mainly with water and showing weaker interaction with the framework. The data indicate that exchange efficiency and site selectivity depend on cation size and on its hydration shell. After  $\text{NH}_4^+$  further exchange Y, which vacates in site IV while retaining a minor presence in I', appears more labile and poorly retained compared to the other REEs, highlighting the importance of the hydration shell of Y in the exchange mechanism, in fact, in site IV Y was bonded only with water molecules and not directly with the zeolite framework as the other REEs. Electron balance analyses from XRPD, SEM-EDS, TG, and EA indicate consistency in most samples. Discrepancies in site occupancies are largely compensated by water molecules, suggesting mixed occupancies for the sites.

### CONCLUSIONS

This research demonstrated the potential of  $\text{NH}_4$ -exchanged zeolite 13X for selectively recovering REEs (Ce, La, Eu, Y). The zeolite maintained its exchange capacity under mildly acidic conditions and showed high affinity for Ce and La, and low for Y. Further tests are required for Eu since the behaviour seems influenced by starting concentrations. Mono-elemental exchange tests revealed Ce and La reached exchange plateaus at moderate liquid-to-solid ratios, while Y, despite its higher concentration, exchanged less efficiently. Structural analysis confirmed Ce, La, and Eu cations directly bond to the framework at defined sites, whereas Y resides in the supercage, weakly bound to water, explaining its easier recovery upon  $\text{NH}_4^+$  counter-exchange and less overall



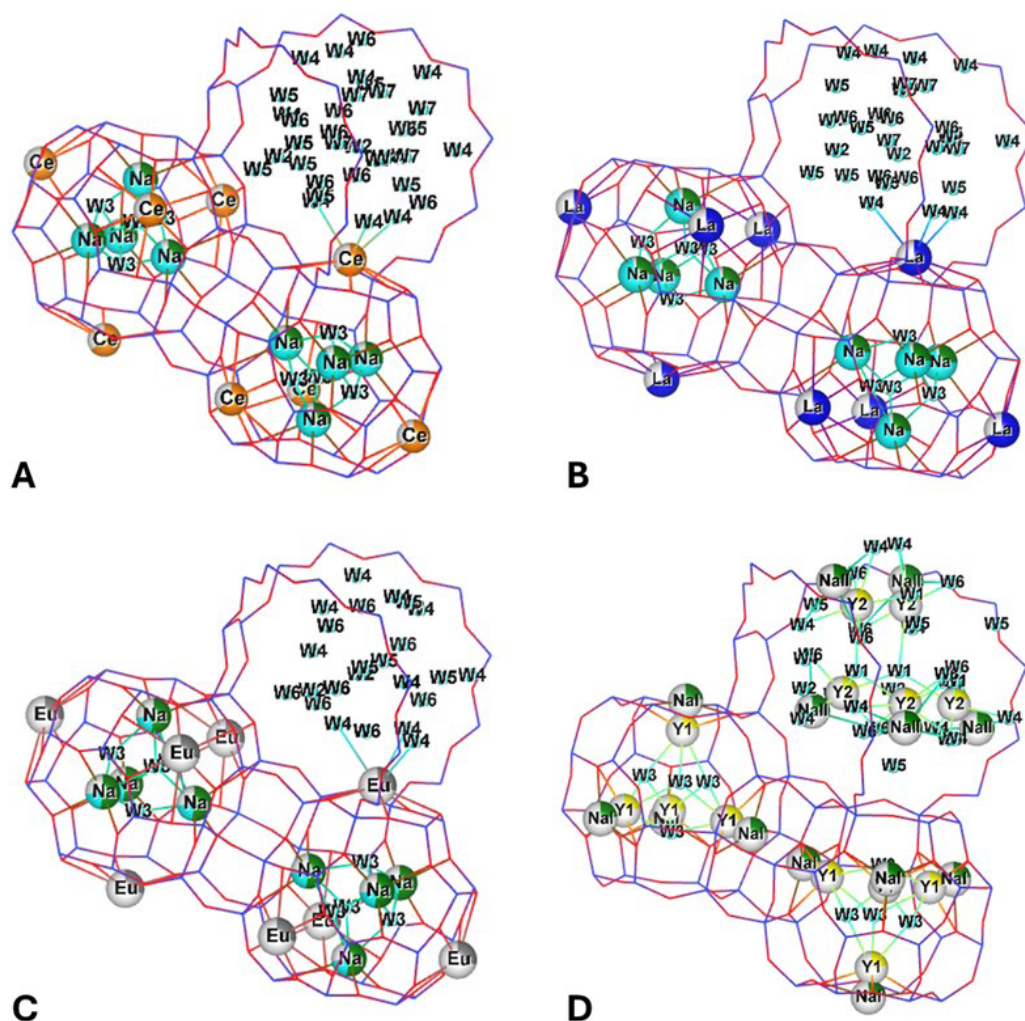


**Figure 3** a) graphical representation of the zeolite framework, with cations (Ce in orange, Na in green) and water molecules (in light blue). b) graphical representation of the zeolite framework, with cations (La in blue, Na in green) and water molecules (in light blue). c) graphical representation of the zeolite framework, with cations (Eu in grey, Na in green) and water molecules (in light blue). d) graphical representation of the zeolite framework, with cations (Y in yellow, Na in green) and water molecules (in light blue).

exchange capacity. Bi-elemental tests further highlighted the zeolite's selectivity, particularly in separating Y from Eu. Only Y was significantly recovered in these tests, while Ce, La, and Eu remained strongly retained. The presence of residual Na may have influenced exchange behaviours, suggesting future work should focus on full  $\text{NH}_4$  substitution. Overall,  $\text{NH}_4$ -13X shows promise for REE separation, especially Y, and selective retention of Ce and La, with potential implications for REE recycling and recovery from complex waste streams.

## REFERENCES

- Borst, A., Smith, M.P., Finch, A., Estrade, G., Villanova-de-Benavent, C., Nason, P., Marquis, E., Horsburgh, N.J., Goodenough, K., Xu, C., Kyniky, J., Geraki, K. (2020) - Adsorption of rare earth elements in regolith-hosted clay deposits. *Nat. Commun.*, 11, 4386.
- Castor, S.B. (2008) - Rare Earth Deposits of North America. *Resour. Geol.*, 58(4), 337-47.
- Dushyantha, N., Batapola, N., Ilankoon, I.M.S.K., Rohitha, S., Premasiri, R., Abeyasinghe, B., Ratnayake, N., Dissanayake, K. (2020) - The story of rare earth elements (REEs): Occurrences, global distribution, genesis, geology, mineralogy and global production. *Ore Geol. Rev.*, 122, 103521.
- Eduafo P.M., Strauss M.L., Mishra B. (2015) - Experimental investigation of recycling rare earth metals from waste fluorescent lamp phosphors. In: "Rare Metal Technology 2015", N. R. Neelameggham, S. Alam, H. Oosterhof, A. Jha, D. Dreisinger, S. Wang, eds. Springer, Cham, 253-259.
- Feng, X., Onel, O., Council-Troche, M., Noble, A., Yoon, R., Morris, J.R. (2021) - A study of rare earth ion-adsorption clays: The speciation of rare earth elements on kaolinite at basic pH. *Appl. Clay Sci.*, 201.
- Frising, T. & Leflaive, P. (2008) - Extraframework cation distributions in X and Y faujasite zeolites: A review. *Micropor. Mesopor. Mat.*, 114(1), 27-63.
- Grohol, M. & Veeh, C. (2023) - Study on the critical raw materials for the EU 2023, Final report.
- U. S. Geological Survey (2024) - Mineral commodity summaries 2024, Report: 212 pp.
- Huang, X. W., Zhou, M. F., Qiu, Y. Z., Qi, L. (2015) - In-situ LA-ICP-MS trace elemental analyses of magnetite: The Bayan Obo Fe-REE-Nb deposit, North China. *Ore Geol. Rev.*, 65, 884-99.
- Jaireth, S., Hoatson, D. M., Miezeitis, Y. (2014) - Geological setting and resources of the major rare-earth-element deposits in Australia. *Ore Geol. Rev.*, 62, 72-128.

- Lottermoser, B.G. & England, B.M. (1988) - Compositional variation in pyrochlores from the Mt Weld carbonatite laterite, Western Australia. *Mineral. Petrol.*, 38(1), 37-51.
- Lottermoser B.G. (1990) - Rare-earth element mineralisation within the Mt. Weld carbonatite laterite, Western Australia. *Lithos*, 24(2), 151-67.
- Smith, M.P., Moore, K., Kavecsánszki, D., Finch, A.A., Kynicky, J., Wall, F. (2016) - From mantle to critical zone: A review of large and giant sized deposits of the rare earth elements. *Geosci. Front.*, 7(3), 315-34.
- Song, W., Xu, C., Smith, M.P., Chakhmouradian, A.R., Brenna, M., Kynický, J., Chen, W., Yang, Y., Deng, M., Tang H. (2018) - Genesis of the world's largest rare earth element deposit, Bayan Obo, China: Protracted mineralization evolution over ~1 b.y. *Geology*, 46(4), 323-6.
- Vogt, E.T.C. & Weckhuysen, B.M. (2015) - Fluid catalytic cracking: recent developments on the grand old lady of zeolite catalysis. *Chem. Soc. Rev.*, 44(20), 7342-70.